

5

Parallel Shear Flow: the Effects of Viscosity

We now imagine a parallel shear flow in a fluid that is homogeneous but has nonzero viscosity ν (e.g., Figure 5.1). Recall from section 1.5 that ν is treated as a constant and can represent either molecular viscosity or an effective viscosity due to turbulence.

In the presence of viscosity, the divergence equation is unchanged from (1.17):

$$\vec{\nabla} \cdot \vec{u} = 0. \quad (5.1)$$

The momentum equation (1.19), neglecting buoyancy but retaining viscosity, is

$$\frac{D\vec{u}}{Dt} = -\vec{\nabla}\pi + \nu\nabla^2\vec{u}. \quad (5.2)$$

The viscosity term raises the order of the system and therefore requires additional boundary conditions. These will be discussed in detail below (section 5.4). For the moment we'll just observe that a viscous fluid must move with the boundary, so for a stationary boundary $u = v = w = 0$.

5.1 Conditions for Equilibrium

Consider a parallel shear flow

$$\vec{u} = U(z)\hat{e}^{(x)}, \quad (5.3)$$

with pressure $\Pi(x, y, z)$. As in Chapter 3, gravity is irrelevant, so z is not necessarily the vertical coordinate. The parallel flow (5.3) satisfies the divergence equation, and its material derivative is zero. Substituting into (5.2) and separating the components, we have

$$\frac{\partial \Pi}{\partial x} = \nu \frac{\partial^2 U}{\partial z^2} \quad (5.4)$$

$$\frac{\partial \Pi}{\partial y} = \frac{\partial \Pi}{\partial z} = 0 \quad (5.5)$$



Figure 5.1 Kelvin-Helmholtz instability in paleo-earthquakes revealed in sediment deformations near the Dead Sea. The billow amplitude is ~ 1 m. These deformations can be modeled by the flow of a viscous fluid. Adapted from Heifetz et al. (2005).

Evidently the pressure gradient is arranged so as to balance the force of viscosity acting on the mean flow. We will call this **frictional equilibrium**.

According to (5.5), Π can be at most a function of x .¹ Equation (5.4) therefore requires that a function of x equal a function of z , which is possible only if both are constant. A parallel shear flow that is steady in a viscous fluid must therefore obey

$$\frac{d^2U}{dz^2} = \text{const.} \quad (5.6)$$

The velocity profile $U(z)$ can take one of three forms: (i) a quadratic function of z if the constant is nonzero, (ii) a linear function if the constant is zero, or (iii) zero, which we examined in Chapter 2. An immediate consequence of (5.6) is that d^2U/dz^2 cannot change sign, i.e., there is no inflection point. In the absence of viscosity, this class of flows would be stable. We consider two examples.

Plane Poiseuille flow: A parallel flow driven by a constant pressure gradient is a quadratic function. With stationary boundaries at $z = 0$ and $z = H$, U has the form

$$U(z) = 4u_0 \frac{z}{H} \left(1 - \frac{z}{H}\right), \quad (5.7)$$

where u_0 is the maximum velocity, found at $z = H/2$ (Figure 5.2a). The effect of viscosity is balanced by a constant pressure drop in the x direction:

$$\frac{d\Pi}{dx} = -8\nu \frac{u_0}{H^2}.$$

Plane Poiseuille flow has a cylindrical counterpart, the classical engineering problem of flow in a pipe.

Plane Couette flow: If there is no pressure gradient, the velocity profile is a linear function. One way to power a flow in this circumstance is to have one boundary move relative to the other, e.g.,

¹ Compare this with the inviscid case, section 3.1.1, where $v = 0$ and therefore Π is uniform.

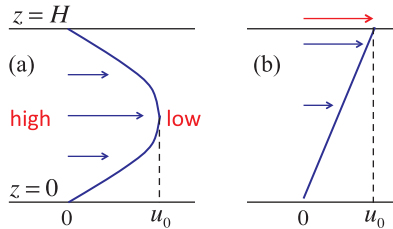


Figure 5.2 Equilibrium states in a viscous fluid. (a) Plane Poiseuille flow maintained by a uniform pressure gradient. (b) Plane Couette flow driven by a moving upper boundary.

$$U(z) = u_0 \frac{z}{H}.$$

In this case the boundary at $z = H$ moves at speed u_0 and the boundary at $z = 0$ is stationary (Figure 5.2b).

5.2 Conditions for Quasi-Equilibrium: the Frozen Flow Approximation

If the mean flow is *not* in equilibrium, we cannot use our methods of stability analysis, because the normal mode solution (3.14) is invalid when the coefficients of the equations are functions of time. So, channeling our inner child, we ask, “But can we do it if the mean flow is *almost* in equilibrium?” The answer is yes, we can, if we’re very careful.

Suppose that the mean flow is not exactly in equilibrium; it is evolving slowly, perhaps under the action of viscosity. Suppose also that an instability grows rapidly, so that it reaches large amplitude before the mean flow has time to change very much. We can guess, then, that the evolution of the mean flow will have little effect on the instability. On that basis, we can do the stability analysis with normal modes just as if the mean flow were steady. This is called the **frozen flow approximation**. But, we must check afterward to make sure that the growth rate really is fast enough to justify the approximation.

Suppose that the mean velocity profile $U(z)$ can be characterized by a length scale h and a velocity scale u_0 . Suppose further that it diffuses under the action of viscosity on a time scale T . Now assume that there is no pressure gradient to force the flow; it’s just diffusing freely:

$$\frac{\partial U}{\partial t} = \nu \frac{\partial^2 U}{\partial z^2}. \quad (5.8)$$

We can estimate the terms in this equation as follows:

$$\frac{u_0}{T} = \nu \frac{u_0}{h^2},$$

or

$$T = \frac{h^2}{\nu}.$$

Now if

$$\sigma T \gg 1, \quad (5.9)$$

then the instability will grow by many factors of e in the time it takes the mean flow to diffuse. Suppose, for example, that the instability is a shear instability, so its growth rate scales like

$$\sigma = \sigma^* \frac{u_0}{h}.$$

Then the condition $\sigma T \gg 1$ is equivalent to

$$\sigma^* \gg \frac{\nu}{u_0 h},$$

or

$$\boxed{\sigma^* \gg \frac{1}{Re}}, \quad (5.10)$$

where

$$\boxed{Re = \frac{u_0 h}{\nu}} \quad (5.11)$$

is the **Reynolds number**. Any solution we obtain that does not satisfy (5.10) must be interpreted with great caution.

5.3 The Orr-Sommerfeld Equation

We now substitute perturbation forms

$$\vec{u} = U(z)\hat{e}^{(x)} + \epsilon \vec{u}' ; \quad \pi = \Pi(x) + \epsilon \pi'$$

into the equations of motion (5.1) and (5.2). The procedure is similar to the inviscid case, which we examined in detail in section 3.1.2; we have only to account for the added term representing viscosity in the momentum equation.

Viscosity makes no difference to the divergence condition (3.5):

$$\vec{\nabla} \cdot \vec{u}' = 0. \quad (5.12)$$

Because there is no nonlinearity in the viscous term, the momentum equation is just (3.7) with an extra term:

$$\frac{\partial \vec{u}'}{\partial t} + U(z) \frac{\partial \vec{u}'}{\partial x} + w' \frac{dU}{dz} \hat{e}^{(x)} = -\vec{\nabla} \pi' + \nu \nabla^2 \vec{u}'. \quad (5.13)$$

To obtain the Poisson equation for the pressure, we again take the divergence of the momentum equation. Because the divergence of the added viscosity term is zero by (5.12), the result is exactly the same as (3.11):

$$\nabla^2 \pi = -2U_z \frac{\partial w'}{\partial x}.$$

We now substitute the pressure equation into the Laplacian of the vertical component of (5.13). The result is just (3.12) with the added viscosity term:

$$\frac{\partial}{\partial t} \nabla^2 w' + U \frac{\partial}{\partial x} \nabla^2 w' = U_{zz} \frac{\partial w'}{\partial x} + \nu \nabla^4 w'. \quad (5.14)$$

Substituting the normal mode form (3.14) now gives the **Orr-Sommerfeld equation**:

$$\sigma \nabla^2 \hat{w} = -ikU \nabla^2 \hat{w} + ikU_{zz} \hat{w} + \nu \nabla^4 \hat{w}, \quad (5.15)$$

where

$$\nabla^2 = \frac{d^2}{dz^2} - \tilde{k}^2; \quad \tilde{k}^2 = k^2 + \ell^2.$$

This may also be written in terms of the phase speed, $c = i\sigma/k$:

$$(U - c) \nabla^2 \hat{w} = U_{zz} \hat{w} - \frac{i\nu}{k} \nabla^4 \hat{w}. \quad (5.16)$$

In the special case $\nu = 0$, this is equivalent to the Rayleigh equation (3.18).

The viscous case differs from the inviscid case in a very important way. Recall that, in the inviscid case, phase velocities occur in complex conjugate pairs so that every decaying mode is accompanied by a growing mode (section 3.4). If all modes are neutral, i.e., $c_i = 0$, or $\sigma_r = 0$, we say that the flow is **Lyapunov stable**, meaning that the flow remains near the equilibrium state but does not return to it. In the viscous equation (5.16), one term has a complex coefficient, so that c need not occur in complex conjugate pairs. It is possible (common, in fact) for all modes to have $c_i < 0$, or $\sigma_r < 0$. Physically, this means that all perturbations are dissipated by viscosity. Mathematically, we may say that such a flow is **asymptotically stable** (it eventually returns to equilibrium), or **exponentially stable**, since departures from equilibrium decay at an exponential rate.

5.4 Boundary Conditions for Viscous Fluid

As usual we assume impermeable boundaries $w' = 0$ (cf. 3.39) above and below the region of interest. But because the Orr-Sommerfeld equation (5.15) is fourth-order (it contains fourth derivatives in the viscous term), two more boundary conditions are needed. These correspond to additional assumptions about the nature of the boundary. There are two plausible choices: solid and frictionless.

5.4.1 The Solid (No-Flow) Boundary

This is the most obvious choice. Physically, we know that velocity goes to zero at a boundary, because fluid molecules become intermingled with the boundary molecules. In the case of a moving boundary, the flow velocity approaches the boundary velocity. Here, we'll assume stationary boundaries, but the generalization to a moving boundary is trivial. So not only is $w' = 0$ at the boundaries, but u' and v' are zero also.

We're not done yet, though. These additional conditions pertain to u' and v' , but for (5.15) we need conditions on w' . We arrange this as follows. Because $u' = 0$ everywhere on the boundary, and in particular for all values of x , it also follows that $\partial u'/\partial x = 0$ everywhere on the boundary. Likewise, because $v' = 0$ for all y , $\partial v'/\partial y = 0$. Substituting these results into the divergence condition:

$$\frac{\partial u'}{\partial x} + \frac{\partial v'}{\partial y} + \frac{\partial w'}{\partial z} = 0,$$

we find that $\partial w'/\partial z = 0$. When working with normal modes, the added condition at a **solid boundary** is

$$\hat{w}_z = 0, \quad (5.17)$$

where the subscript indicates the z -derivative.

5.4.2 The Frictionless Boundary

In most flows, the retarding effect of viscosity is restricted to a thin layer adjacent to the boundary within which the velocity goes rapidly to zero. This is called the **viscous boundary layer**. Outside the viscous boundary layer, the velocity changes much more slowly; the fluid slips past as if the boundary were frictionless.

If the region of interest is much larger than the viscous boundary layer, we can pretend that the outer edge of the layer is actually the boundary, and impose the condition $\partial u'/\partial z = \partial v'/\partial z = 0$ at that location. An equivalent way to state this is that the viscous momentum fluxes $-\nu \partial u'/\partial z$ and $-\nu \partial v'/\partial z$ vanish at the boundary. The boundary may therefore be called “flux-free” (or just “free”).

To convert this condition to a condition on \hat{w} for use in the Orr-Sommerfeld equation (5.15), we use the derivative of the divergence condition. Because $\vec{\nabla} \cdot \vec{u}' = 0$ everywhere in the flow, its z -derivative is also zero:

$$\frac{\partial}{\partial z} \left(\frac{\partial u'}{\partial x} + \frac{\partial v'}{\partial y} + \frac{\partial w'}{\partial z} \right) = \frac{\partial^2 u'}{\partial x \partial z} + \frac{\partial^2 v'}{\partial y \partial z} + \frac{\partial^2 w'}{\partial z^2} = 0.$$

Now since $\partial u'/\partial z = 0$ for all x , $\partial^2 u'/\partial x \partial z = 0$, and by the same reasoning $\partial^2 v'/\partial y \partial z = 0$, leaving us with $\partial^2 w'/\partial z^2 = 0$. In normal mode form, the added condition at a **free slip** (or frictionless) boundary is

$$\hat{w}_{zz} = 0. \quad (5.18)$$

5.5 Numerical Solution of the Orr-Sommerfeld Equation

Write the Orr-Sommerfeld equation in the form (5.15):

$$\sigma \nabla^2 \hat{w} = -\iota k U \nabla^2 \hat{w} + \iota k U_{zz} \hat{w} + \nu \nabla^4 \hat{w},$$

where

$$\nabla^2 = \frac{d^2}{dz^2} - \tilde{k}^2.$$

Possible choices of boundary conditions include

$$\hat{w} = 0; \quad \hat{w}_z = 0 \quad (\text{solid}) \quad (5.19)$$

$$\hat{w} = 0; \quad \hat{w}_{zz} = 0 \quad (\text{free}). \quad (5.20)$$

As in the inviscid case, the Laplacian is represented as a matrix \mathbf{A} :

$$\nabla^2 \rightarrow \mathbf{A} = \mathbf{D}^{(2)} - \tilde{k}^2 \mathbf{I},$$

where $\mathbf{D}^{(2)}$ is the second-derivative matrix incorporating the impermeable boundary condition $\hat{w} = 0$.

Similarly, the right-hand side of the Orr-Sommerfeld equation is expressed using a second matrix, which is just (3.36) with the extra viscous term:

$$\mathbf{B} = -\iota k \vec{U} \cdot \mathbf{A} + \iota k \vec{U}_{zz} \cdot \mathbf{I} + \nu (\mathbf{D}^{(4)} - 2\tilde{k}^2 \mathbf{D}^{(2)} + \tilde{k}^4 \mathbf{I}), \quad (5.21)$$

where $\mathbf{D}^{(4)}$ is a fourth-derivative matrix incorporating the boundary conditions (5.19 or 5.20). With free-free boundary conditions, the fourth-derivative matrix turns out to be equivalent to the square of the second-derivative matrix (try it!). If either boundary is solid, though, the fourth-derivative matrix must be designed separately via Taylor series expansions as described in sections 1.4.2 and 1.4.3.

Consider the usual approximation for the second derivative at $i = 1$:

$$f_1'' \simeq \frac{f_0 - 2f_1 + f_2}{\Delta^2}. \quad (5.22)$$

Instead of $f_0 = 0$, we must now assume that $f'_0 = 0$. That assumption can be expressed using the one-sided approximation to the derivative developed in project 1:

$$f'_0 \simeq \frac{-3f_0 + 4f_1 - f_2}{2\Delta} = 0 \quad \Rightarrow f_0 = \frac{4f_1 - f_2}{3}$$

Substituting this into (5.22), we have

$$f_1'' \simeq \frac{-2f_1 + 2f_2}{3\Delta^2}$$

and the top line of the matrix is therefore $[-2/3 \ 2/3 \ \dots]/\Delta^2$. For $i = N$, the result is

$$f_N'' \simeq \frac{2f_{N-1} - 2f_N}{3\Delta^2}.$$

Left-multiplications are performed as in section 3.5.2. The Orr-Sommerfeld equation now becomes a generalized eigenvalue problem:

$$\sigma \mathbf{A}\vec{w} = \mathbf{B}\vec{w},$$

which can be solved using standard numerical functions.

5.6 Oblique Modes

As we have discussed in sections 3.7 and 4.3, every oblique mode has a corresponding 2D mode. If the oblique mode has wave vector (k, ℓ) , then the corresponding 2D mode has wave vector $(\tilde{k}, 0)$ as shown in Figure 3.10. The growth rates are σ and $\tilde{\sigma}$, respectively. We found that, in the absence of viscosity, the growth rates are related by $\sigma = \cos \varphi \tilde{\sigma}$, where φ is the angle of obliquity. Here we will see how viscosity affects that relationship.

We begin by writing the Orr-Sommerfeld equation (5.15) more explicitly:

$$(\sigma + ikU) \left(\frac{d^2}{dz^2} - \tilde{k}^2 \right) \hat{w} = ikU_{zz} \hat{w} + v \left(\frac{d^2}{dz^2} - \tilde{k}^2 \right)^2 \hat{w}. \quad (3D)$$

Suppose we have a solution algorithm for this equation:

$$\sigma = \mathcal{F}(z, U, v; k, \ell). \quad (5.23)$$

This equation and solution algorithm pertain to any mode, an oblique mode in particular.

For a corresponding 2D mode, having wave vector $(\tilde{k}, 0)$, (3D) becomes

$$(\sigma + i\tilde{k}U) \left(\frac{d^2}{dz^2} - \tilde{k}^2 \right) \hat{w} = i\tilde{k}U_{zz} \hat{w} + v \left(\frac{d^2}{dz^2} - \tilde{k}^2 \right)^2 \hat{w}, \quad (2D)$$

with solution algorithm

$$\sigma = \mathcal{F}(z, U, v; \tilde{k}, 0). \quad (5.24)$$

Now we start again with (3D) and make the Squire transformations $k = \tilde{k} \cos \varphi$ and $\sigma = \tilde{\sigma} \cos \varphi$ (as we did in the inviscid case; section 3.7), and

$$\nu = \tilde{\nu} \cos \varphi.$$

Substituting these into (3D) and dividing out $\cos \varphi$, we have

$$(\tilde{\sigma} + i\tilde{k}U) \left(\frac{d^2}{dz^2} - \tilde{k}^2 \right) \hat{w} = i\tilde{k}U_{zz}\hat{w} + \tilde{\nu} \left(\frac{d^2}{dz^2} - \tilde{k}^2 \right)^2 \hat{w}. \quad (3\widetilde{D})$$

The form (3 \widetilde{D}) is isomorphic to the special case (2D):

$$(3\widetilde{D}) \leftrightarrow (2D), \text{ under } \tilde{\sigma} \rightarrow \sigma \text{ and } \tilde{\nu} \rightarrow \nu.$$

This means that we can use the same solution algorithm as for the 2D case (5.24):

$$\tilde{\sigma} = \mathcal{F}(z, U, \tilde{\nu}; \tilde{k}, 0),$$

or

$$\sigma = \cos \varphi \times \mathcal{F}(z, U, \frac{\nu}{\cos \varphi}; \tilde{k}, 0).$$

As in the inviscid case, a general 3D mode with $\varphi \neq 0$ and growth rate σ corresponds to a 2D mode ($\varphi = 0$) whose growth rate is reduced to $\sigma \cos \varphi$. But there is another important difference: **the corresponding 2D mode grows on a flow with increased viscosity $\tilde{\nu} = \nu / \cos \varphi$.**

It is often true that viscosity has the effect of *damping* instability, as we have seen in the convection case (Chapter 2). If that is true, the tendency of 2D modes to grow faster than the corresponding 3D modes is increased by this heightened sensitivity to viscosity. However, it is not impossible that viscosity could act to destabilize a flow. If that were true, and if that viscous destabilization was sufficient to overcome the leading factor $\cos \varphi$, then a 3D mode could grow faster than the corresponding 2D mode.

5.7 Shear Scaling and the Reynolds Number

Here again is the Orr-Sommerfeld equation (3D):

$$(\sigma + ikU) \left(\frac{d^2}{dz^2} - \tilde{k}^2 \right) \hat{w} = ikU_{zz}\hat{w} + \nu \left(\frac{d^2}{dz^2} - \tilde{k}^2 \right)^2 \hat{w}, \quad (3D)$$

with solution algorithm

$$(\sigma, \hat{w}) = \mathcal{F}(z, U, \nu; k, \ell).$$

(Note that we have included the eigenfunction \hat{w} in the output of \mathcal{F} . Previously, this was omitted for simplicity only.)

For shear scaling, we define a length scale h and a velocity scale u_0 , just as in section 3.6. For example, the familiar hyperbolic tangent shear layer

$$U = u_0 \tanh \frac{z}{h}$$

can be written as

$$U^* = \tanh z^*,$$

where

$$U^* = \frac{U}{u_0}; \quad z^* = \frac{z}{h},$$

(reproducing 3.47). Other quantities can be scaled as in (3.51), also reproduced here for convenience:

$$\begin{aligned} \sigma &= \sigma^* \frac{u_0}{h} \\ \{k, \ell, \tilde{k}\} &= \{k^*, \ell^*, \tilde{k}^*\}/h \\ \hat{w} &= \hat{w}^* u_0 \\ \frac{d}{dz} &= \frac{1}{h} \frac{d}{dz^*} \quad \Rightarrow \nabla^2 = \frac{1}{h^2} \left(\frac{d^2}{dz^{*2}} - \tilde{k}^{*2} \right). \end{aligned}$$

With these substitutions, the Orr-Sommerfeld equation (3D) can be rewritten as

$$(\sigma^* + ik^* U^*) \left(\frac{d^2}{dz^{*2}} - \tilde{k}^{*2} \right) \hat{w}^* = ik^* U_{z^* z^*}^* \hat{w}^* + \frac{\nu}{hu_0} \left(\frac{d^2}{dz^{*2}} - \tilde{k}^{*2} \right)^2 \hat{w}^*, \quad (3D*)$$

The scaled viscosity appearing in the second term on the right-hand side is the inverse of the Reynolds number (5.11). (3D*) is isomorphic to (3D) and therefore has the same solution algorithm under the shear scalings listed above:

$$(\sigma^*, \hat{w}^*) = \mathcal{F}(z^*, U^*, 1/Re; k^*, \ell^*). \quad (5.25)$$

5.8 Numerical Examples

5.8.1 Viscous Stabilization of a Shear Layer

Consider a hyperbolic tangent shear layer $U^* = \tanh z^*$ in a viscous fluid (e.g., Figure 5.1). In the limit $Re \rightarrow \infty$, viscosity is negligible and the instability is indistinguishable from that found in an inviscid fluid (section 3.9.1). As Re is reduced, the effects of viscosity become evident (Figure 5.3). The growth rate of the fastest-growing mode decreases, and its wavelength increases. (As in the case of convective instability, larger-scale disturbances are better able to resist viscous damping.) The flow is completely stabilized when $Re = 2.7$. That number should be taken with a large grain of salt, however, since the condition $\sigma^* \gg 1/Re$ is not satisfied.

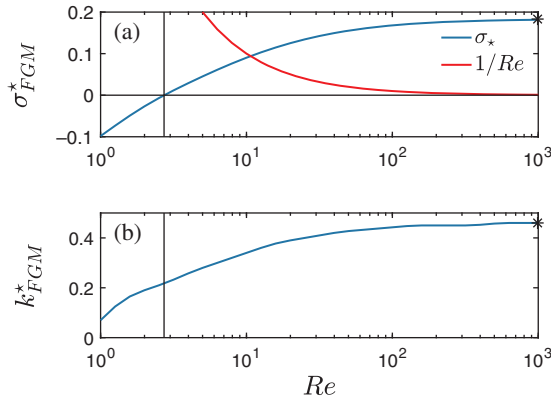


Figure 5.3 Stability characteristics of a hyperbolic tangent shear layer $U^* = \tanh z^*$ in a viscous fluid. Frictionless boundaries are placed at $z^* = \pm 5$. (a) Fastest growth rate of shear layer instability versus Re . The red curve indicates $1/Re$. (b) Wavenumber of fastest-growing mode. Asterisks show the inviscid result (e.g., Figure 3.12).

A useful and valid rule of thumb² that we can extract from this analysis is that viscous effects become important when Re drops below ~ 100 . Suppose, for example, that the shear layer at the base of the ocean mixed layer is 10 m thick, and the velocity change across it is 0.1 m/s, so that $h = 5$ m and $u_0 = 0.05$ m/s. In that case, the condition $Re < 100$ is equivalent to $\nu > 2.5 \times 10^{-4}$ m²/s. That value is in the normal range for turbulent viscosity at the mixed layer base, and we should therefore expect that shear instability in this regime will be affected significantly by ambient turbulence.

5.8.2 Instabilities of Plane Poiseuille Flow

Here we use the matrix-based numerical approach to explore the instabilities of plane Poiseuille flow (5.7; Figure 5.2), which is one of the few shear flows that are truly steady in a viscous fluid. In shear-scaled terms, the mean flow profile is

$$U^* = 4z^*(1 - z^*). \quad (5.26)$$

We begin by setting the spanwise wavenumber ℓ^* to zero and looking at the growth rate as a function of streamwise wavenumber k^* for a range of Reynolds numbers. A distinct region of instability is found (Figure 5.4), with maximum growth rate at $Re = 10^5$. This is called the **Tollmien-Schlichting instability**. In this case the fastest-growing mode has $k^* = 1.55$, or wavelength about 4 times the width of the channel.

² “It’s more of a guideline than a rule.” Bill Murray in *Ghostbusters*.

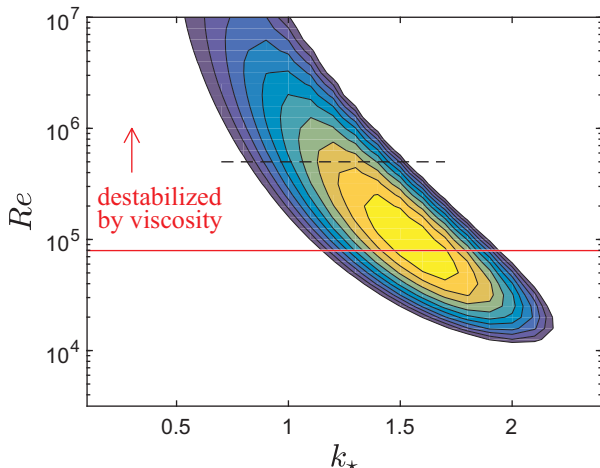


Figure 5.4 Stability characteristics of plane Poiseuille flow (5.26). Colors indicate the growth rate versus wavenumber k^* and Reynolds number Re for 2D modes $\ell^* = 0$. For $Re > 8 \times 10^4$ (above the red line), the growth rate decreases with increasing Re or, in other words, increases with increasing viscosity. The dashed line pertains to Figure 5.6.

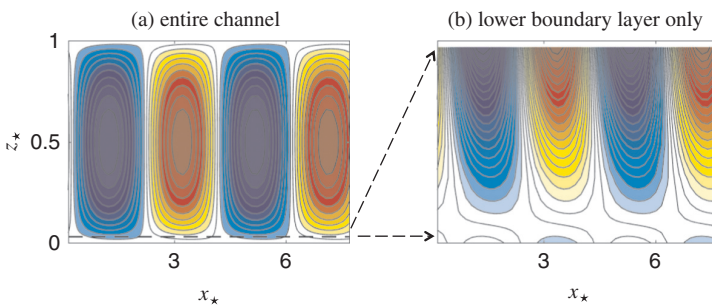


Figure 5.5 Vertical velocity perturbation for the Tollmien-Schlichting instability of plane Poiseuille flow. (a) The entire vertical domain. (b) Blowup of the lower region bounded by the dashed line in (a), showing the up-shear phase tilt.

For $Re > 10^5$, the maximum growth rate increases with decreasing Re , i.e., with increasing viscosity. This is therefore an example of a mode that is destabilized by viscosity. In the absence of viscosity (the limit $Re \rightarrow \infty$), the growth rate is zero.

Contours of the cross-stream (or wall-normal) velocity perturbation (Figure 5.5) show that isolines tilt against the background shear near the boundaries. It is this aspect of the perturbation that allows it to access energy from the mean flow despite the absence of an inflection point.

The fact that the Tollmien-Schlichting mode is destabilized by viscosity raises the possibility that the fastest-growing instability may be oblique (on the basis of Squire's theorem). In Figure 5.6, we show a test of this possibility for a value

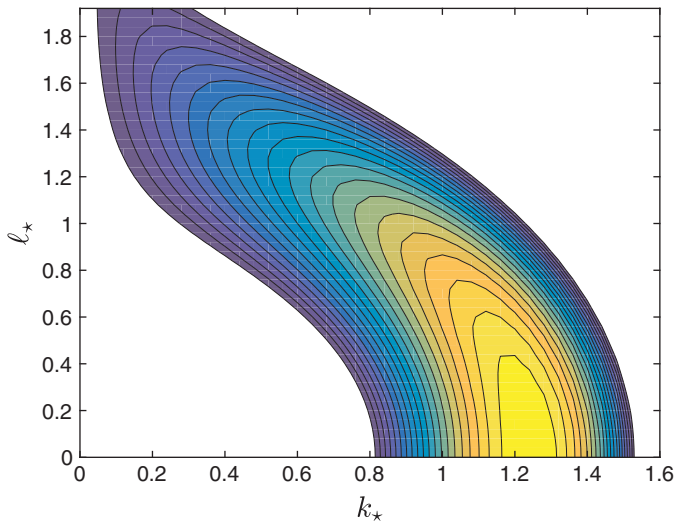


Figure 5.6 Growth rates of oblique modes of plane Poiseuille flow versus scaled wavenumber. $Re = 5 \times 10^5$, indicated in Figure 5.4 by the dashed line. Growth is maximized in the 2D limit despite the destabilizing role of viscosity.

$Re = 5 \times 10^5$, well into the region where the growth rate increases with increasing viscosity (Figure 5.4). The fastest-growing mode is in fact two-dimensional; all oblique modes have lower growth rates.

Test your understanding: Is the criterion $\sigma^* \gg 1/Re$ relevant for plane Poiseuille flow?

5.9 Perturbation Energetics in Viscous Flow

When exploring the inviscid case, we derived the kinetic energy equation in terms of real perturbation variables u' , w' , etc., which represent a general disturbance (section 3.10.1). We then applied the result to a normal mode perturbation by integrating quadratic combinations over one wavelength (section 3.10.2). Here we will repeat the derivation with viscous terms included, and we'll allow for fully three-dimensional modes ($\ell \neq 0$). And, just for variety, we'll do the math in normal mode form right from the start.

As in the inviscid case, the perturbation equations describing continuity and momentum are given by (5.12) and (5.13). In normal mode form, these can be written as:

$$\imath k \hat{u} + \imath \ell \hat{v} = -\hat{w}_z, \quad (5.27)$$

$$(\sigma + \imath k U) \hat{u} = -U_z \hat{w} - \imath k \hat{\pi} + \nu \nabla^2 \hat{u} \quad (5.28)$$

$$(\sigma + \imath k U) \hat{v} = -\imath \ell \hat{\pi} + \nu \nabla^2 \hat{v} \quad (5.29)$$

$$(\sigma + \imath k U) \hat{w} = -\hat{\pi}_z + \nu \nabla^2 \hat{w} \quad (5.30)$$

where the subscript z indicates the derivative. We now multiply the momentum equations, (5.28), (5.29), and (5.30), by the complex conjugates of the velocity eigenfunctions, \hat{u}^* , \hat{v}^* , and \hat{w}^* , respectively, and add the results:

$$\overbrace{(\sigma + \imath k U) (|\hat{u}|^2 + |\hat{v}|^2 + |\hat{w}|^2)}^{(1)} = \overbrace{-U_z \hat{u}^* \hat{w}}^{(2)} - \overbrace{\imath k \hat{u}^* \hat{\pi} + \imath \ell \hat{v}^* \hat{\pi}}^{(3)} - \overbrace{\hat{w}^* \hat{\pi}_z}^{(4)} + \nu (\hat{u}^* \nabla^2 \hat{u} + \hat{v}^* \nabla^2 \hat{v} + \hat{w}^* \nabla^2 \hat{w}). \quad (5.31)$$

Next, we take the real part of each term.

- (1) The real part of the left-hand side is $4\sigma_r K$, where

$$K = \frac{|\hat{u}|^2 + |\hat{v}|^2 + |\hat{w}|^2}{4} \quad (5.32)$$

is the perturbation kinetic energy (cf. 3.65).

- (2) The real part is twice the shear production (cf. 3.66):

$$SP = -\frac{U_z}{2} (\hat{u}^* \hat{w})_r.$$

- (3) The first two terms of (3) can be written as

$$(-\imath k \hat{u}^* - \imath \ell \hat{v}^*) \hat{\pi}.$$

The sum in parentheses is equal to $(\imath k \hat{u} + \imath \ell \hat{v})^*$, which is equal to $-\hat{w}_z^*$ by (5.27). Therefore, (3) can be rewritten as

$$-\hat{w}_z^* \hat{\pi} - \hat{w}^* \hat{\pi}_z = -(\hat{w}^* \hat{\pi})_z.$$

After taking the real part, the quantity in parentheses is twice the energy flux (cf. 3.67):

$$EF = \frac{(\hat{w}^* \hat{\pi})_r}{2},$$

so that the real part of (3) is $-2EF_z$.

- (4) The fourth term is due to viscosity. It can be split into two parts, which represent distinct physical processes. The three terms in the parentheses of term (4) all have the same form, which can be rewritten as follows:

$$\begin{aligned} \hat{u}^* \nabla^2 \hat{u} &= \hat{u}^* \hat{u}_{zz} - \tilde{k}^2 \hat{u}^* \hat{u} \\ &= (\hat{u}^* \hat{u}_z)_z - \hat{u}_z^* \hat{u}_z - \tilde{k}^2 \hat{u}^* \hat{u} \\ &= (\hat{u}^* \hat{u}_z)_z - |\hat{u}_z|^2 - \tilde{k}^2 |\hat{u}|^2 \end{aligned}$$

We now take the real part. The only complex term on the right-hand side is the first one, and its real part is the derivative of

$$(\hat{u}^* \hat{u}_z)_r = \frac{1}{2} (\hat{u}^* \hat{u}_z + \hat{u} \hat{u}_z^*) = \frac{1}{2} (\hat{u}^* \hat{u})_z = \frac{|\hat{u}|_z^2}{2},$$

so we have

$$(\hat{u}^* \nabla^2 \hat{u})_r = \frac{|\hat{u}|_{zz}^2}{2} - |\hat{u}_z|^2 - \tilde{k}^2 |\hat{u}|^2. \quad (5.33)$$

Adding the corresponding terms involving \hat{v} and \hat{w} , we can now assemble term (4):

$$2K_{zz} - |\hat{u}_z|^2 - |\hat{v}_z|^2 - |\hat{w}_z|^2 - 4\tilde{k}^2 K.$$

Collecting all four terms of (5.31) and dividing by 2, we have the kinetic energy equation for normal modes in a viscous shear flow:

$$\boxed{2\sigma_r K = SP - EF_z + \nu K_{zz} - \varepsilon.} \quad (5.34)$$

The final term is minus the viscous dissipation rate

$$\boxed{\varepsilon = \frac{\nu}{2} \left(|\hat{u}_z|^2 + |\hat{v}_z|^2 + |\hat{w}_z|^2 + 4\tilde{k}^2 K \right).} \quad (5.35)$$

The new terms we have gained via the addition of viscosity (and obliquity) are as follows.

- The perturbation kinetic energy (5.32) now includes the third velocity term, $|\hat{v}|^2$.
- The term νK_{zz} is the convergence of a kinetic energy flux due to viscosity, namely $-\nu K_z$.
- The dissipation term $-\varepsilon$ is negative definite and therefore destroys perturbation kinetic energy (converting it to heat).

None of the viscous processes can create perturbation kinetic energy. The viscous flux $-\nu K_z$, like the pressure-driven flux EF , vanishes at the boundaries (check!). So it spreads energy around but does not contribute to the net amount. The dissipation term $-\varepsilon$ is negative definite, and hence can only reduce the kinetic energy. This is a paradox reminiscent of the case of stable stratification (section 4.9). Viscous flows have instabilities that do not exist in the absence of viscosity, e.g., the Tollmien-Schlichting instability, even though viscosity itself acts only as an energy sink for the perturbation. Because viscosity forces the total velocity \vec{u} to go to zero at the boundaries, the perturbation is distorted such that lines of constant w' tilt against the background shear (Figure 5.5) and SP is therefore positive as shown in section 3.11.4. In other words, while viscosity does not create perturbation kinetic energy directly, it configures the perturbation so that it can extract kinetic energy from the mean flow despite the absence of an inflection point.

5.10 Summary

- A parallel shear flow in a viscous fluid can be in equilibrium if either
 - the mean shear is uniform, so that U does not diffuse (as in Couette flow), or
 - viscous smoothing is balanced by a pressure gradient in the x -direction (as in Poiseuille flow).
- The frozen flow approximation permits the use of normal modes provided that the instability grows rapidly compared with the time scale of viscous alteration of the mean profile.
- The Orr-Sommerfeld equation is solved numerically in a manner similar to the Rayleigh equation, but an extra boundary condition (either solid or frictionless) is needed.
- Except in unusual cases, the fastest-growing mode is 2D.
- The effect of viscosity is expressed by the Reynolds number, Re . Viscosity acts to damp shear instability when Re is less than ~ 100 .
- Viscosity can *create* shear instability – not directly, but by forcing the disturbance to obey the solid boundary condition and thereby generating positive shear production.